Supporting Information

Highly Robust, Uniform and Ultra-sensitive Surface-enhanced Raman Scattering Substrates for microRNA Detection Fabricated by Using Silver Nanostructures Assembled in Gold Nanobowls

Taeksu Lee[a,d], Jung-Sub Wi[b], Aram Oh[c], Hee-Kyung Na[b], Jae-Jong Lee[d], Kwangyeol Lee[c], Tae Geol Lee[b,] and Seungjoo Haam[a,]**

Materials and Methods

Preparation of Gold Nanobowls and miR-34a Molecular Beacons (MBs): To prepare the gold nanobowls, a 250-nm-thick film of polymethylglutarimide (PMGI) (PMGI SF5, MicroChem Corp., USA) was first spin-coated on a Si substrate, followed by the spin coating of a 100-nm-thick thermal nanoimprint resist (mr-I 8010R, micro-resist technology GmbH, Germany) layer. The bilayer resist stack was subjected to thermal nanoimprinting at 200 °C under a pressure of 30 bar for 180 s with a commercial tool (ANT-4H, Extech, Korea). We used an array of Si pillars with a 600 nm pitch and 300 nm pillar diameter (Eulitha AG, Switzerland) as the nanoimprint mold. After the nanoimprinting step, the residual nanoimprint resist was etched by O_2 plasma, after which the PMGI resist was wet-etched by a commercial developer solution (AZ MIF300, AZ Electronic Materials, USA) for 3 s. The sample was mounted in a conventional thermal evaporation chamber at an oblique angle (35°) with respect to the evaporation source and continuously rotated (60 rpm) during the deposition to form the bowl-shaped nanostructures. The size of nanobowls in the SEM images, before and after silver deposition, were analyzed via ImageJ program, counting 60 NBs in the each SEM images.

The entire sequences of the molecular beacons for detecting miR-34a were as follows: 5'-HS - TTC GCT GTA CAA CCA GCT AAG ACA CTG CCA-3', 3'-Cy3-GCG ACA TGT TG-5'. In order to prove the site-specificity of the miR-34a beacons, we mutated the five regions (boldfaced in the sequence) in the thiol-modified oligonucleotides as a negative

control: 5'- HS - TTC GCT GTA CAA CC**G** GC**C** AAG AC**G** **T**TG CC**G**-3'. Both the oligomers were mixed in the same molar ratios and annealed at 95 °C for 4 min and then at 70 °C for 10 min, followed by slow cooling to room temperature. All the nucleotides were purchased from Bioneer Inc. (Daejeon, Korea).

Synthesis and Characterization of Silver Nanostructures Grown in Gold Nanobowls (SGBs): Prior to deposition, the gold nanobowl (NB) substrates were rinsed with deionized water thrice. Lacquer was used to passivate the non-reactive areas on the substrates for better fixation of the substrates on the working electrode. This passivation was useful to define the reactive area for the growth of silver nanostructures sin the NBs, with the non-reactive area as a control. Electrochemical experiments were performed using a potentiostat (CompactStat, Ivium) with the conventional three-electrode system employing a Pt wire counter electrode and a Ag/AgCl (1 M KCl) reference electrode. The silver-plating solution was an aqueous solution containing 20 mM silver salt, and its pH was controlled using Na_2CO_3. SGBs were prepared at an overpotential of –1.0 V to –4.0 V using a Ag/AgCl electrode (as a reference electrode) until a charge of –200 mC cm^{-2} passed at room temperature. Thereafter, the polymer resist was removed with excess of acetone (Duksan, Korea) and AZ MIF300 developer solution. The morphology of the SGB was analyzed by FE-SEM (JSM-7001F, JEOL, Japan). In order to measure the nanogap distribution in the synthesized substrates, we selected five SGB3 (SGB synthesized at –3.0 V vs Ag/AgCl) from the SEM images and analyzed at least 25 nanogaps in each SGB3 by ImageJ program. For a more sophisticated analysis, we adjusted the lightness and saturation in the SEM images. The crystal structures of the NB and SGBs were investigated by X-ray diffraction (Ultima3 diffractometer, Rigaku) at room temperature. In addition, the surface elements in the NBs and SGBs were measured using an X-ray photoelectron spectrometer (XPS, K-alpha, Thermo U. K.) with a monochromatic AlK_α X-ray source. The NB and SGB3 were cross sectioned by focused ion

beam milling (FIB, JEOL JIB-4601F, Japan), and elemental analyses of NB and SGB3 were performed using an energy-dispersive X-ray spectrometer (EDS) fitted to a scanning transmission electron microscope (STEM, JEOL JEM-ARM 200F, Japan) The absorption spectra of the rhodamine 6G, Cy3, Cy3 labeled MBs and malachite green isothiocyanate (MGITC) were obtained by using an absorption spectrometer (Mecasys UV-2120).

Surface-enhanced Raman Scattering (SERS) Measurements: Prior to Raman analysis, ethanolic solutions of MGITC (10^{-15} to 10^{-7} M) and rhodamine 6G (10^{-12} and 10^{-3} M) were prepared. The fabricated substrates were immersed in each solution for 4 h and dried overnight. Raman spectroscopy measurements were performed using a confocal Raman microscope (LabRAM ARAMIS, Horiba). To obtain high-quality images, a 100× microscope objective (Nikon, NA = 0.95) and a He-Ne laser (λ = 633 nm) were used. The laser power on the sample was approximately 111 W/mm^2, and the integration time was 10 s. A silicon wafer with a Raman band at 520 cm^{-1} was used as the reference for calibration. LabSpec 5 software (Horiba) was used for spectral and image processing and analysis, including baseline correction. In order to test the stability of synthesized SGB3, two kinds of SGB3 were prepared. MGITC was treated right after SGB3 fabrication, and the Raman dye was added after 3 weeks of SGB3 synthesis. The MGITC was purchased from Fisher Scientific, and rhodamine 6G was obtained from Sigma-Aldrich Korea.

Calculation of SERS Enhancement Factor: The SERS enhancement factors for rhodamine 6G molecules on SGB3 were estimated using the equation:

$$EF = (I_{SGB3}/I_{dye}) \times (N_{dye}/N_{SGB3}), \quad (1)$$

where N_{dye} and N_{SGB3} represent the number of rhodamine 6G molecules on the pure Si substrate (after treatment with 10^{-3} M rhodamine 6G solution) and on the surface of SGB3

(after treatment with 10^{-12} M rhodamine 6G solution), respectively; and I_{dye} and I_{SGB3} are the signal intensities of rhodamine 6G Raman spectra on the pure Si substrate (after treatment with 10^{-3} M rhodamine 6G solution) and on the surface of SGB3 (after 10^{-12} M rhodamine 6G solution).

Conjugation of miR-34a Molecular Beacons (MBs) on SGBs and miR-34a Detection: Prior to conjugation, miR-34a MBs and mutated MBs were mixed with 100 times the high molar ratio of tris(2-carboxyethyl)phosphine (TCEP) overnight. The prepared SGB3 was first immersed in 100 μL of 0.2 μM MBs. The solution was then adjusted with 1 M Tris buffer to obtain a final phosphate concentration of 10 mM (pH 7.2) and with 10% sodium dodecyl sulfate (SDS) solution to obtain a final concentration of 0.1 wt% SDS. The adjusted solution was brought to 0.3 M NaCl by the addition of four aliquots of 2 M NaCl (10 mM Tris, 0.1 % SDS) solution (0.05 M 2 times, 0.1 M 2 times). The MB-hybridized SGB3 were washed thrice with phosphate buffered saline (PBS). In order to detect miR-34a, 100 μL of various concentrations of miR-34a (50 aM to 500 fM) in hybridization buffers (10 mM Tris-HCl, 100 mM KCl, and 1 mM $MgCl_2$, pH 8.0) were reacted with SGB3 for 4 h at 37 °C. The substrate was then rinsed with PBS thrice to remove excess miR-34a and detach the dye molecules, and then dried for SERS detection. The final products were analyzed by Raman spectroscopy (LabRAM ARAMIS, Horiba). For comparison, 500 fM miR-34b and miR-34c samples were analyzed following an identical procedure. Statistical evaluation was performed using analysis of variance (student's t-test), considering $p < 0.03$ statistically significant.

RNA Extraction from MKN-45 and SNU-1 Cell Lines, Quantification of Mature miRNA (miR-34a) Levels Using qRT-PCR, and SERS Detection of miR-34a: Human gastric carcinoma cell lines, SNU-1 and MKN-45, obtained from the Korean Cell Line Bank (KCLB, Korea), were cultured in RPMI1640 medium (Gibco, Invitrogen, Grand Island, NY, USA) supplemented with 10 % fetal bovine serum (FBS) and maintained in a humidified incubator under 5 % CO_2

at 37 °C. SNU-1 cells (suspension cell type) were collected at 1×10^6, and MKN-45 cells were trypsinized and collected at the same cell numbers as that of SNU-1 cell lines. Total RNA was isolated using Trizol (Invitrogen, Carlsbad, CA) according to the manufacturer's protocol, and the isolated total RNA was re-suspended in PBS at 200 ng/μL concentration.

After RNA isolation, we performed the quantification test for mature miR-34a using qRT-PCR. We first isolated total RNA from the SNU-1 and MKN-45 cells using MasterPure™ RNA purification kit (Epicenter). The purity and concentration of all the RNA samples were evaluated by their absorbance ratios at 260/280 nm, determined using a NanoDrop ND-1000 spectrophotometer (NanoDrop Technologies, Rockland, DE, USA).

The expression levels of miRNA (miR-34a, Cat. No. MS00003318, Qiagen) were examined using a SYBR Green method. Reverse transcription of RNA was performed with the miScript Reverse Transcription Kit (Qiagen, Valencia, CA) according to the manufacturer's guidelines. Real-time PCR was performed on a ViiA™ 7 Real-Time PCR System (Applied Biosystems) by the SYBR Green miScript PCR system (Qiagen, Valencia, CA) according to the manufacturer's instructions. Each reaction was performed in a 10 μL volume with 20 ng template cDNA.

All the reactions were run in triplicate. SNORD61 (Cat. No. MS00033705, Qiagen) was used as an endogenous control for the normalization of data. The relative amounts of miR-200a-3p were measured with the $2^{-\Delta\Delta C_T}$ method.

The miR-34a analysis in human cell samples was carried out as follows: miR-34a was extracted from the MKN-45 and SNU-1 cell samples. SERS measurements were conducted after incubating the extracted miR-34a samples with MB-immobilized SGB3 for 2 h. The final products were measured by Raman spectroscopy (LabRAM ARAMIS, Horiba). At least five spectra were obtained from different sites of each sample and averaged to obtain the SERS results.

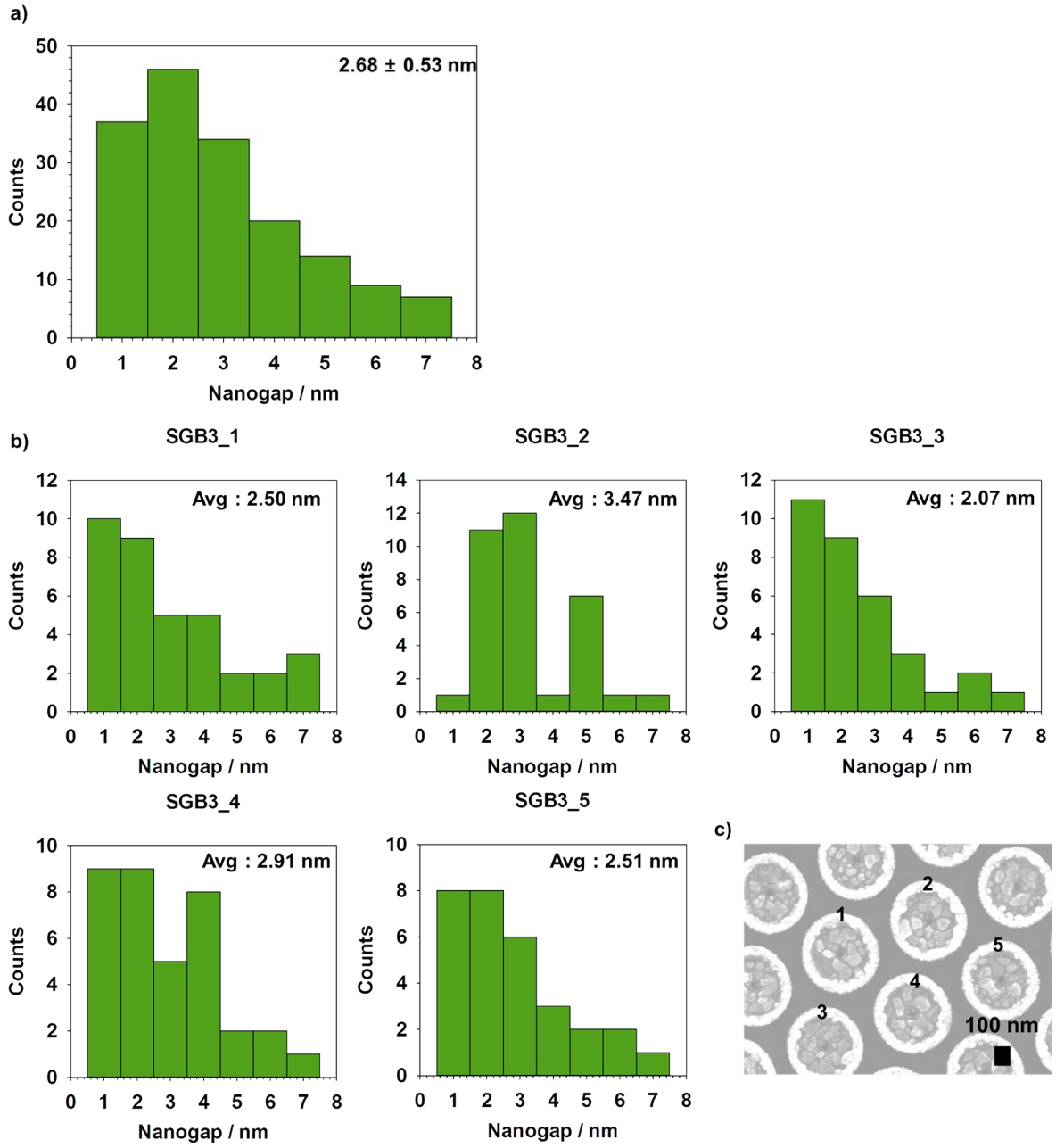

Figure S1. a) Nanogap distribution in five SGB3 and b) nanogap distribution in each SGB3 sample. c) SEM images of SGB3 with optimized brightness and saturation for correct analysis. Nanogaps are measured by ImageJ program.

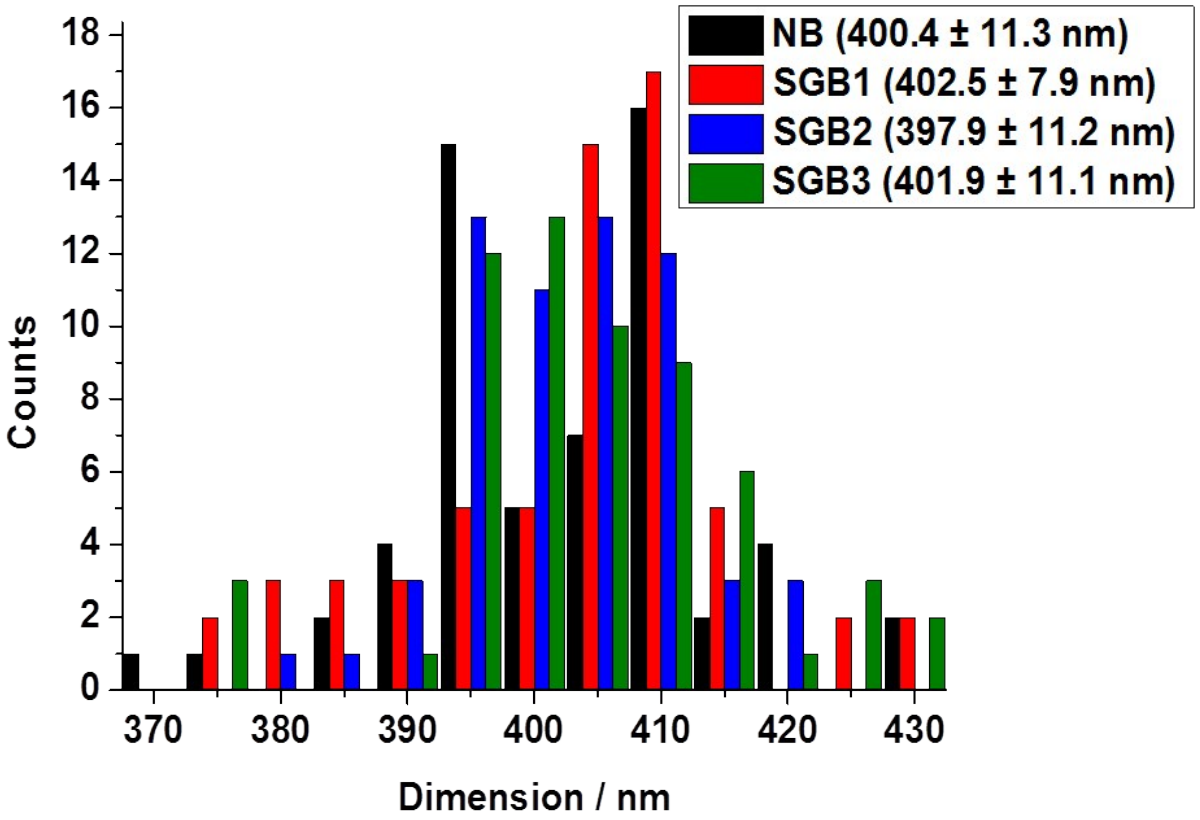

Figure S2. Size distribution of NBs before and after silver nanostructure deposition. The dimensions of NBs in the SEM images (Figure 1) are analyzed by ImageJ program.

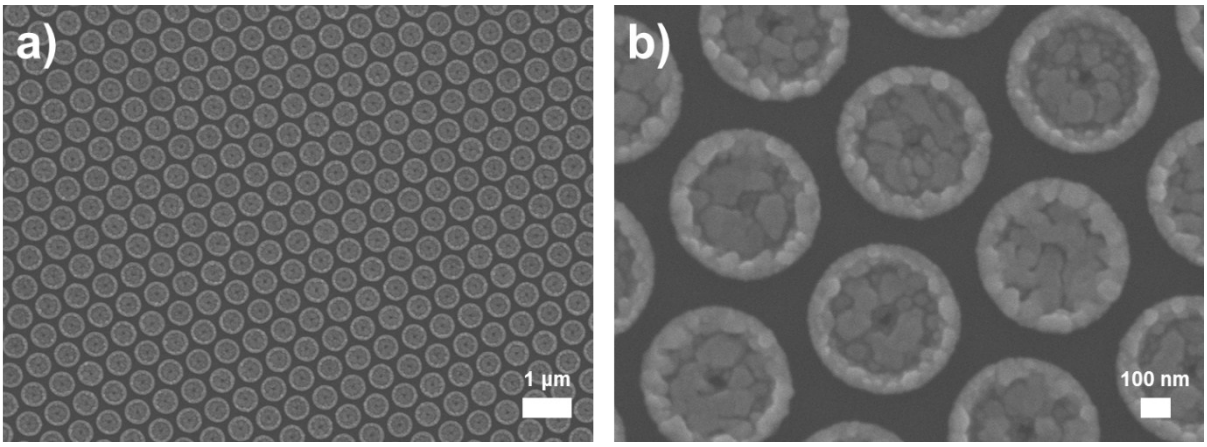

Figure S3. a) SEM image of SGB synthesized at an overpotential of –4.0 V vs Ag/AgCl as a reference electrode and b) its magnified image.

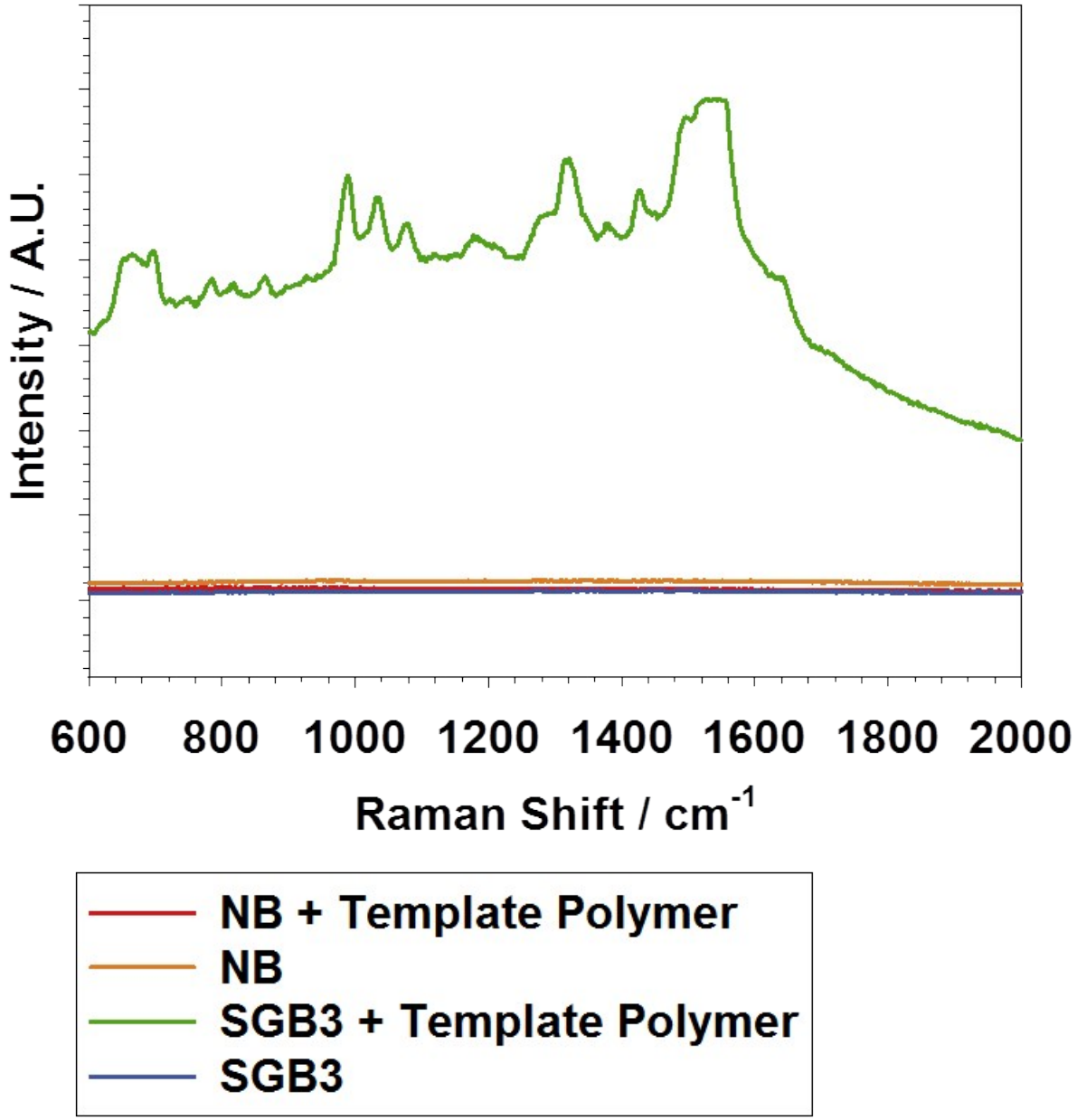

Figure S4. SERS spectra of NB and SGB3 before and after the removal of template polymer.

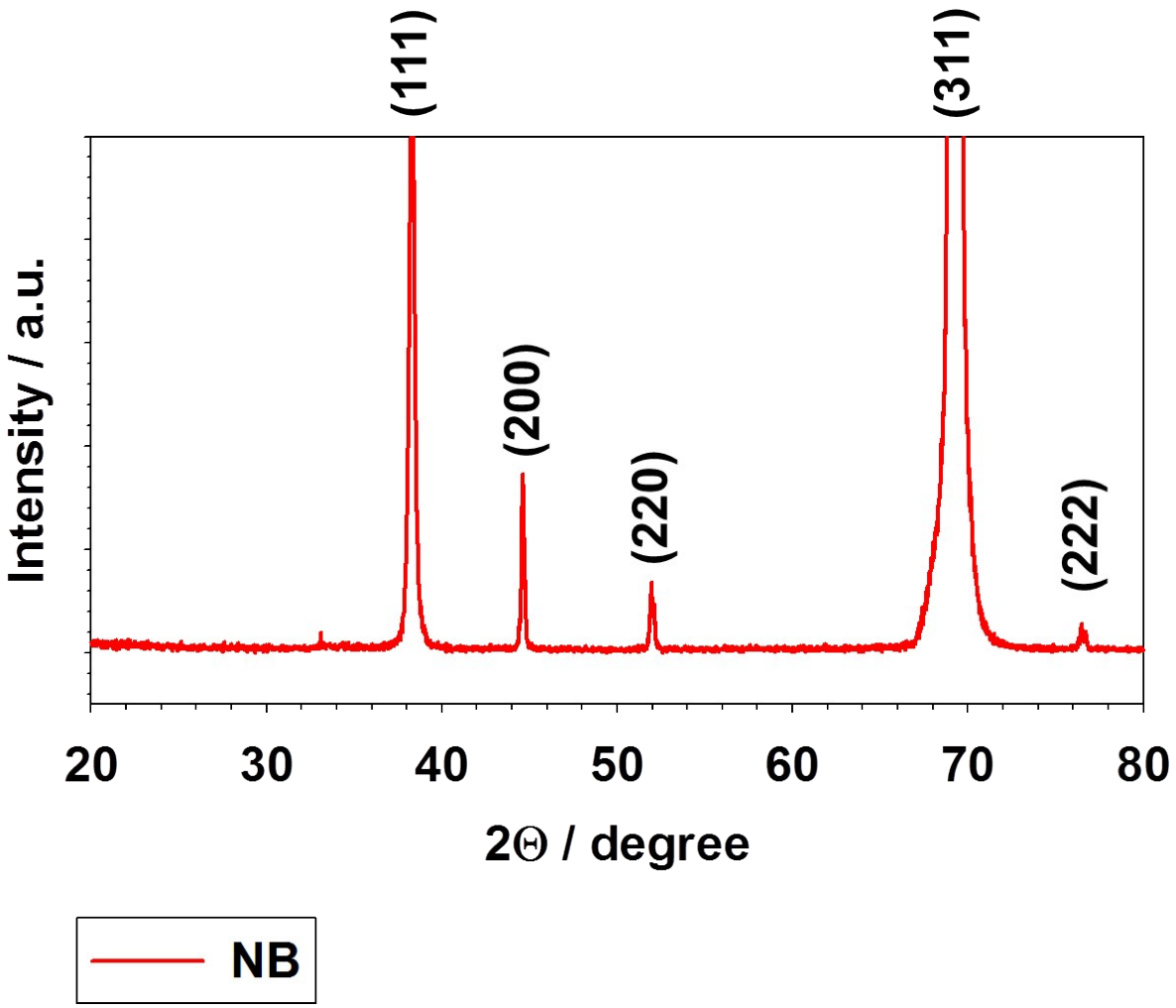

Figure S5. XRD patterns of as-synthesized gold nanobowls.

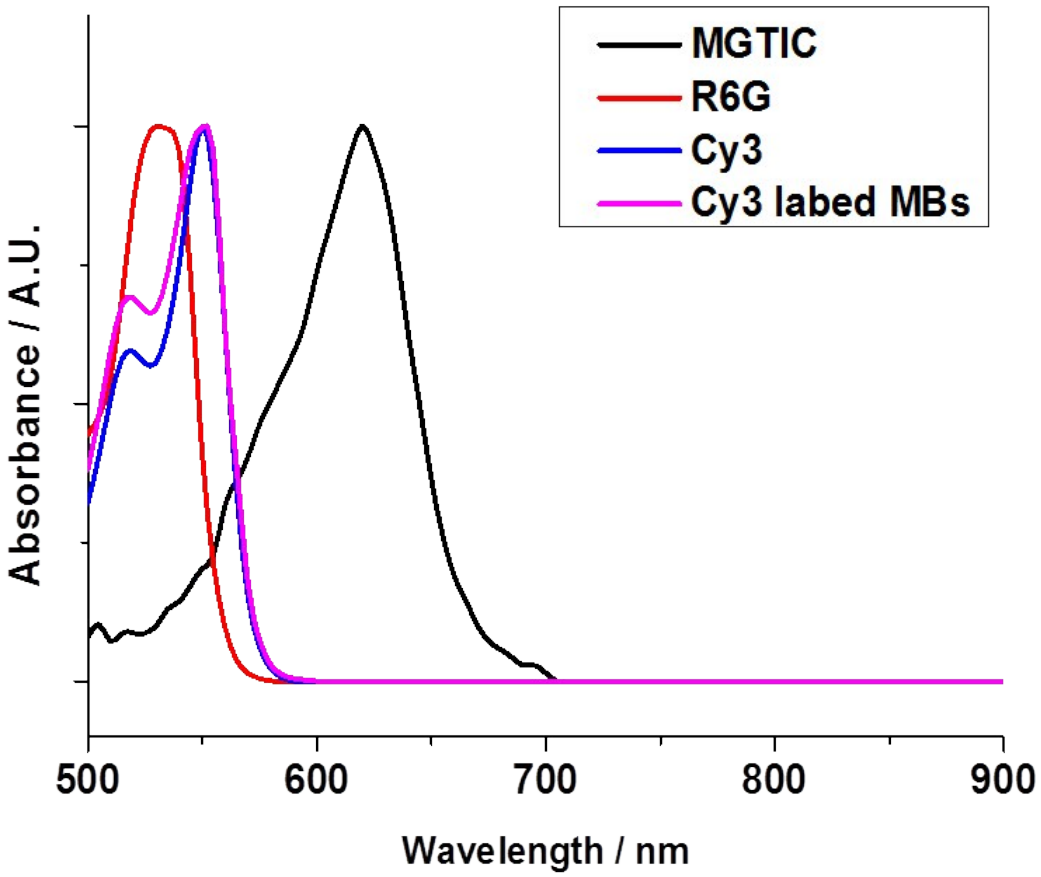

Figure S6. The UV-Vis spectra of MGITC, R6G, Cy3 and Cy3-molecular beacon for detecting miRNA.

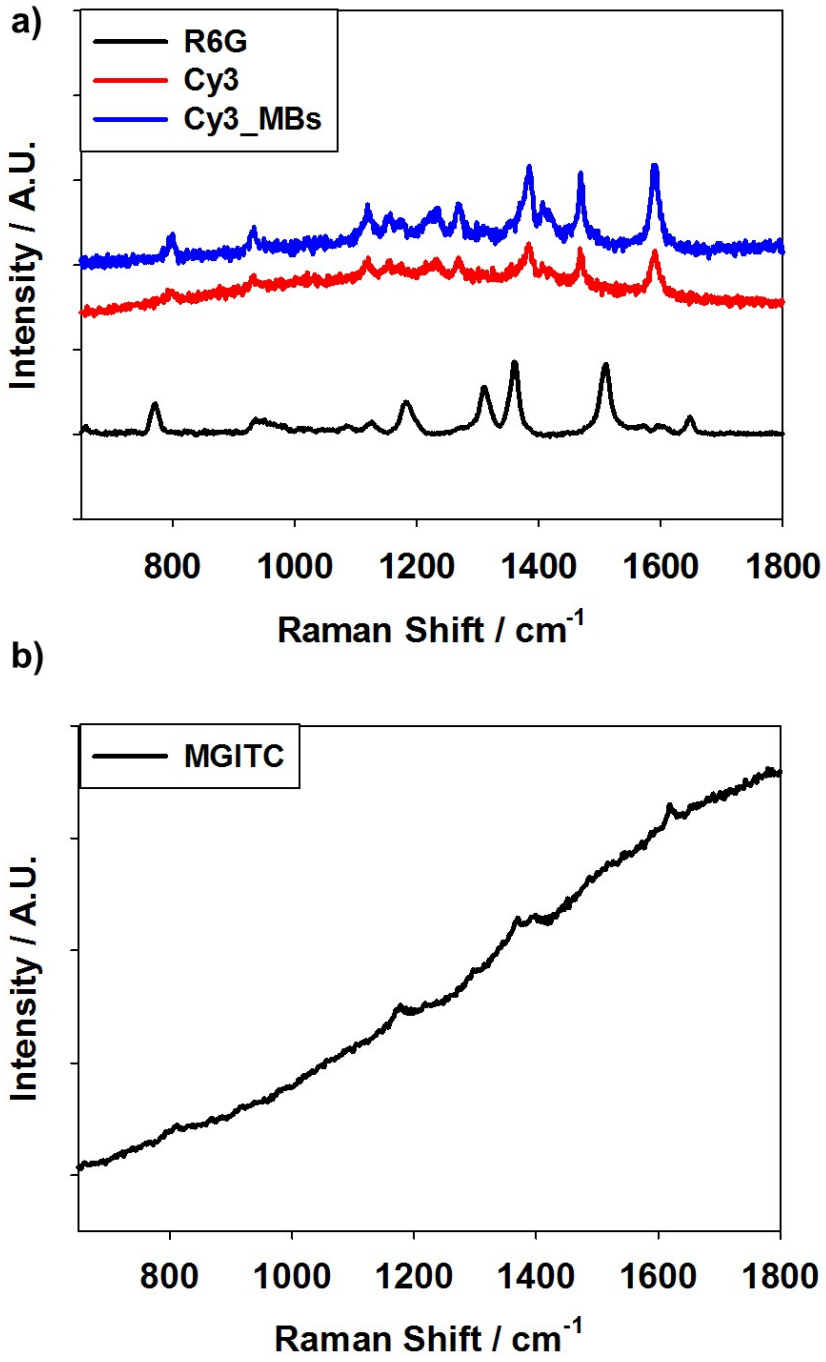

Figure S7. The Raman spectra of a) Cy3 and Cy3-molecular beacon and b) MGITC on bare Si wafer under 633 laser irradiation.

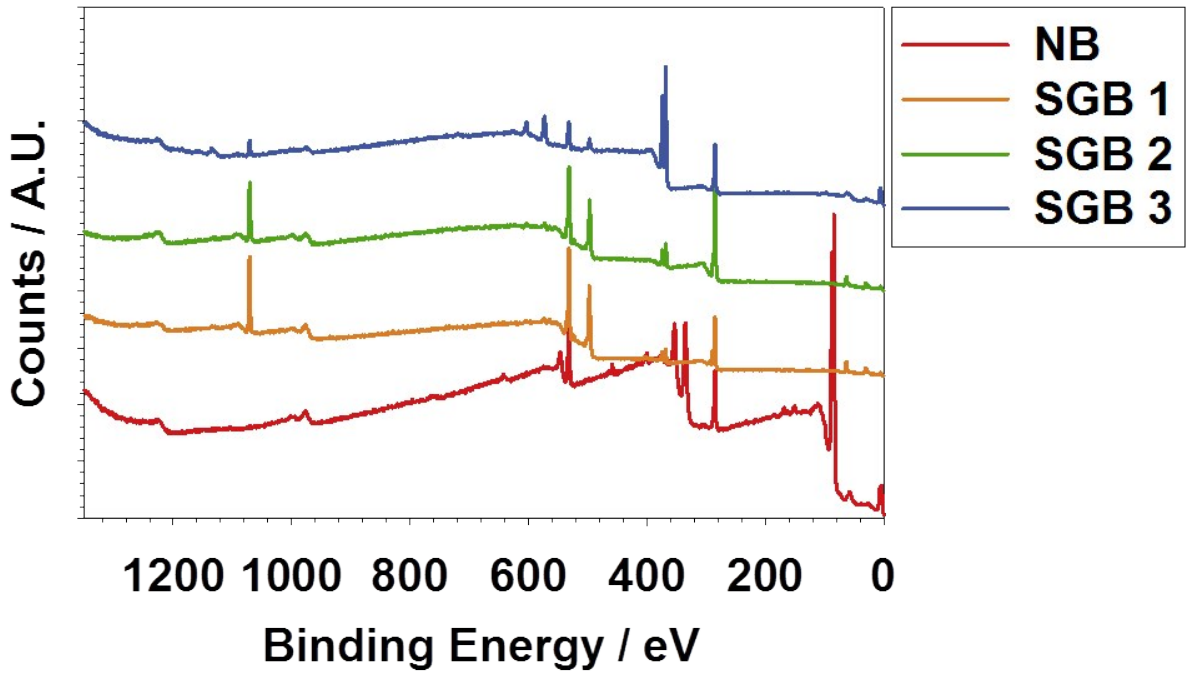

Figure S8. X-ray photoelectron spectra of NB and SGBs.

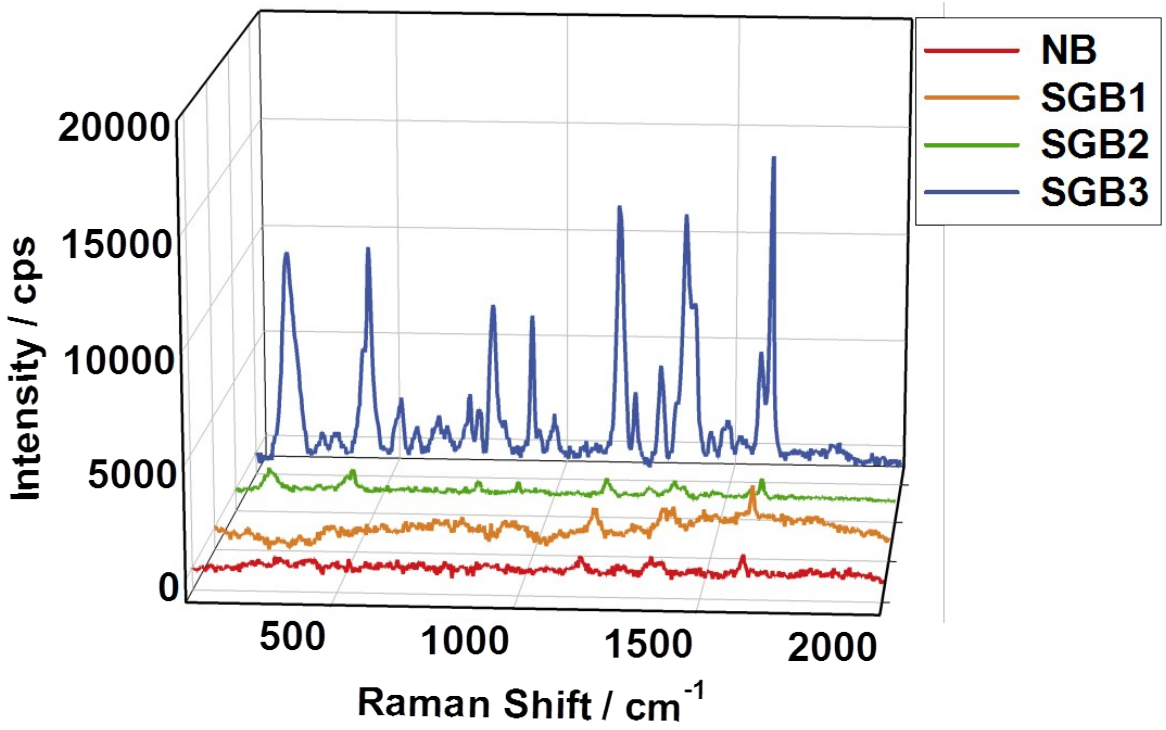

Figure S9. Representative SERS spectra of NB and SGBs under 633 nm laser irradiation after 10^{-7} M of MGITC treatment.

a)

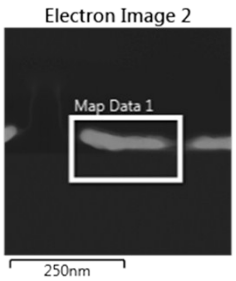

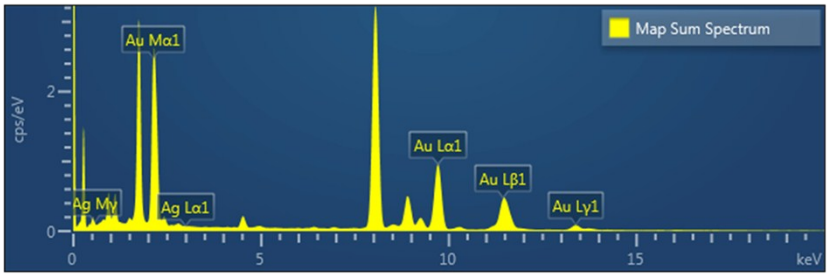

Element	Line Type	k Factor	k Factor type	Absorption Correction	Wt%	Wt% Sigma	Atomic %
Ag	L series	1.079		1.00	0.00	0.00	0.00
Au	L series	0.932		1.00	100.00	0.00	100.00
Total:					100.00		100.00

b)

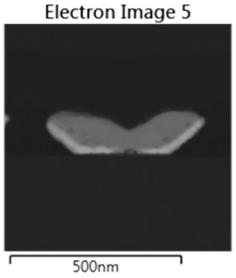

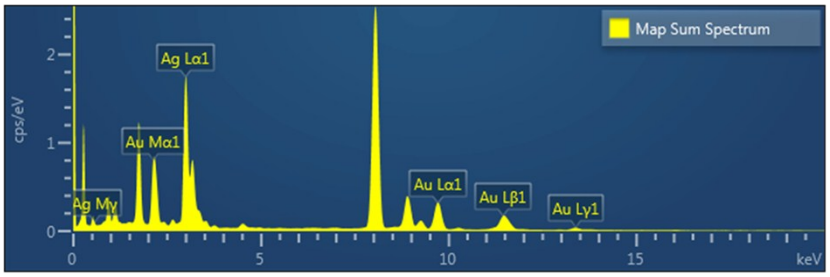

Element	Line Type	k Factor	k Factor type	Absorption Correction	Wt%	Wt% Sigma	Atomic %
Ag	L series	1.079		1.00	76.27	0.55	85.44
Au	L series	0.932		1.00	23.73	0.55	14.56
Total:					100.00		100.00

Figure S10. EDS spectra and calculated atomic ratios of Ag and Au in a) NB and b) SGB3.

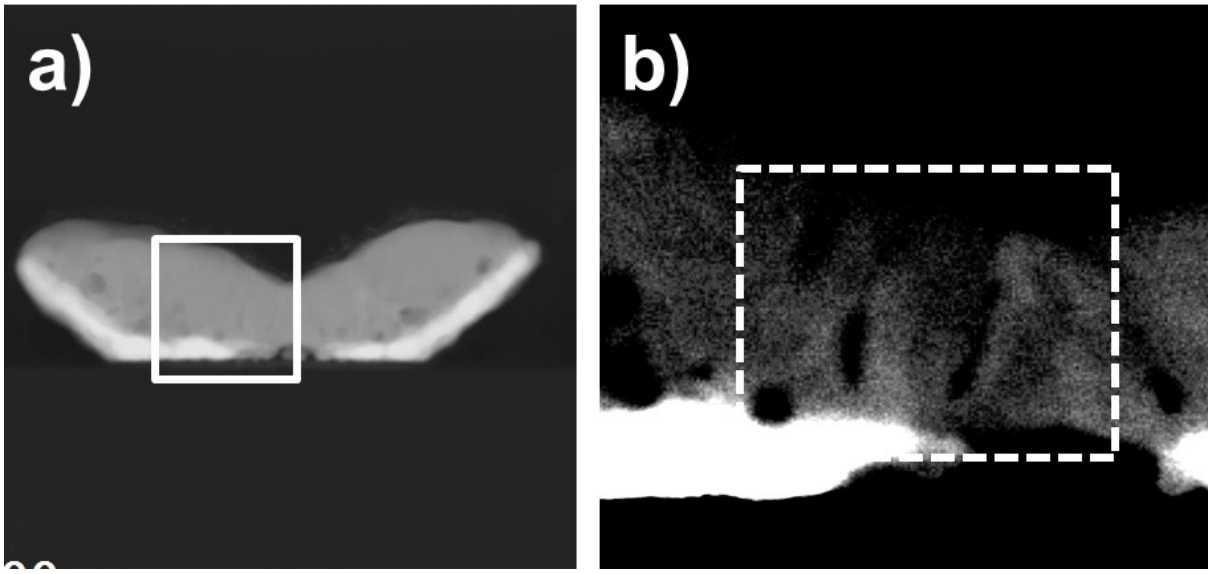

Figure S11. a) STEM image of SGB3 and b) enlarged image of the region enclosed in the white rectangle in a).

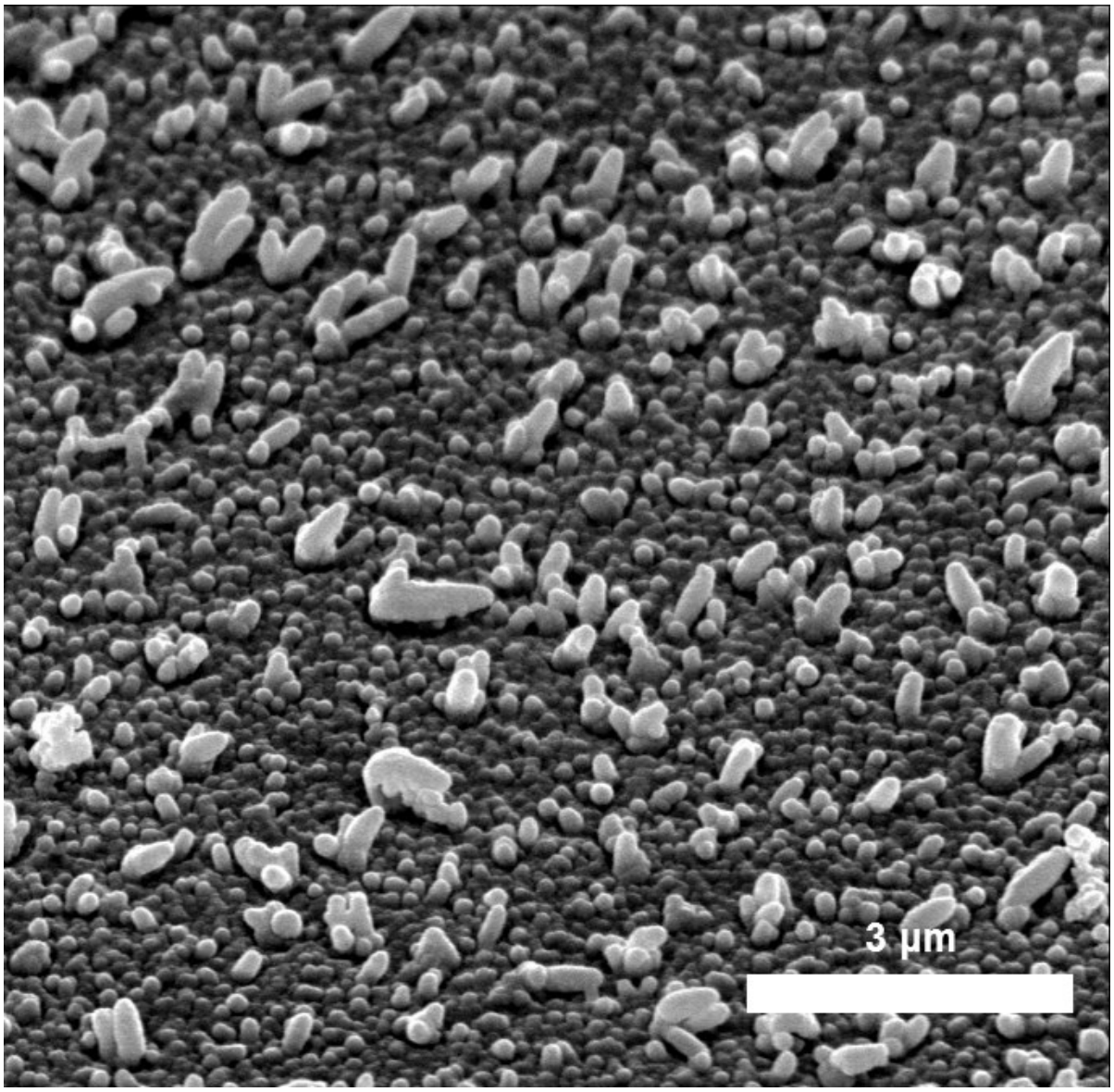

Figure S12. Representative SEM image of silver nanostructures grown without NBs.

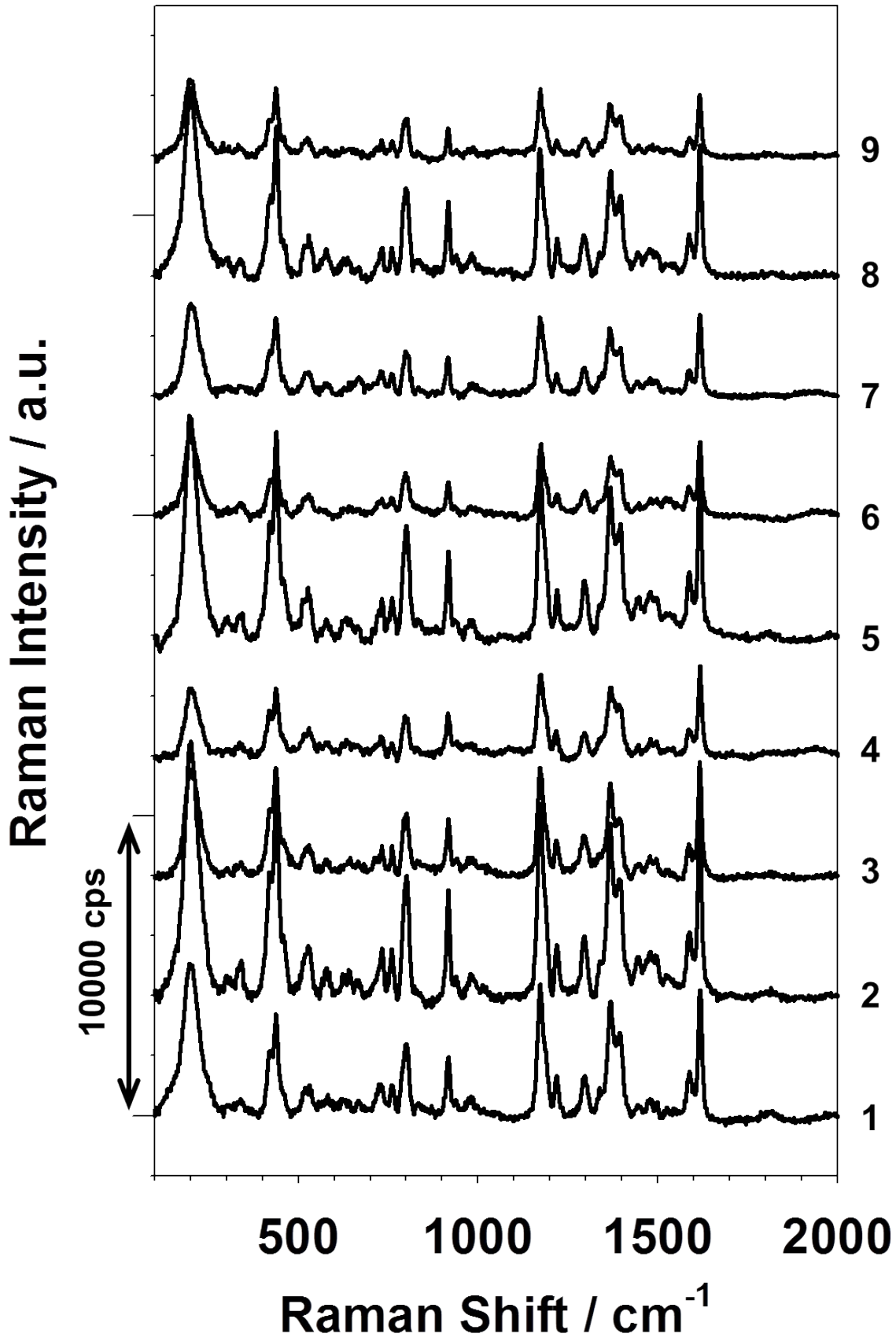

Figure S13. Representative Raman spectra of SN after MGITC treatments.

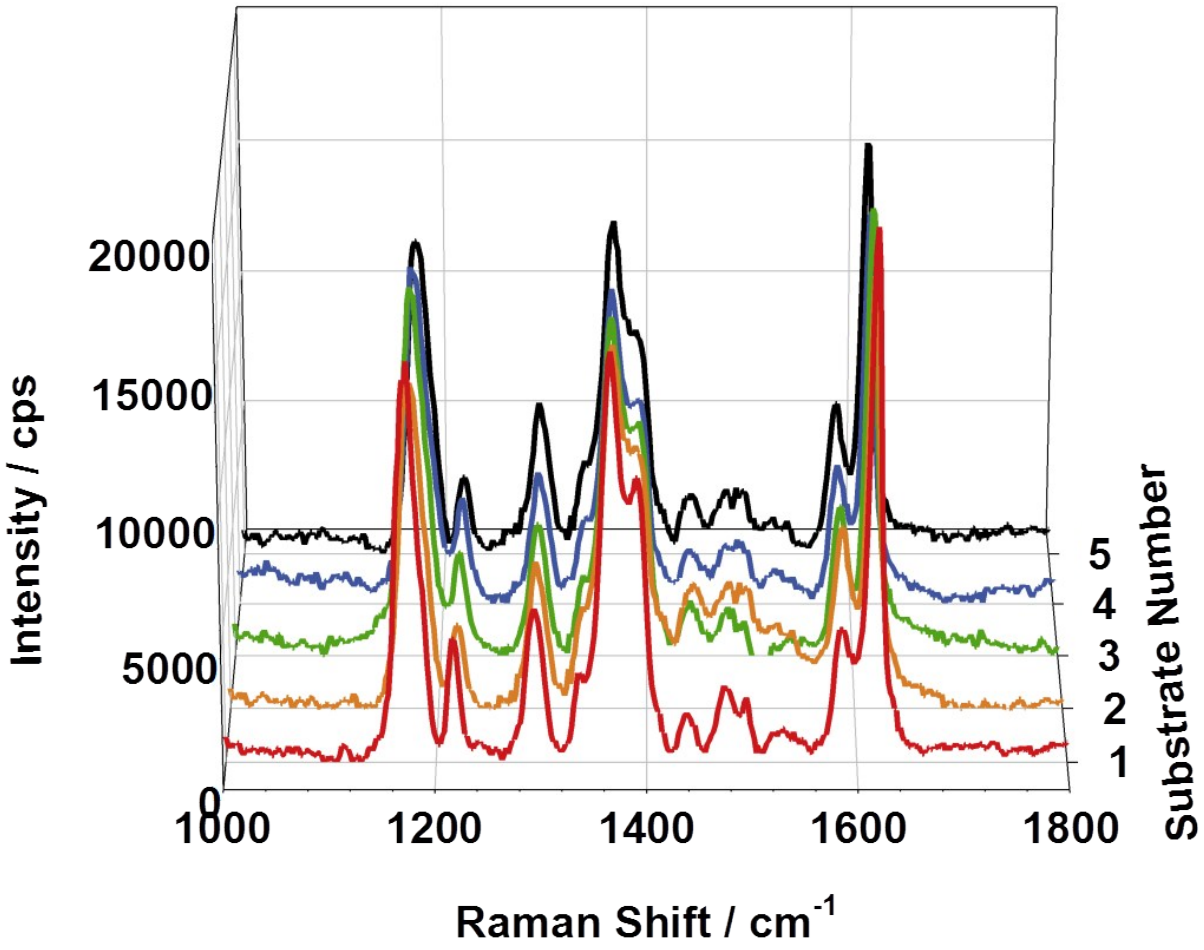

Figure S14. Substrate-to-substrate uniformity of SERS spectra under 633 nm laser irradiation of various SGB3 from 5 different batches after 10^{-7} M of MGITC treatment.

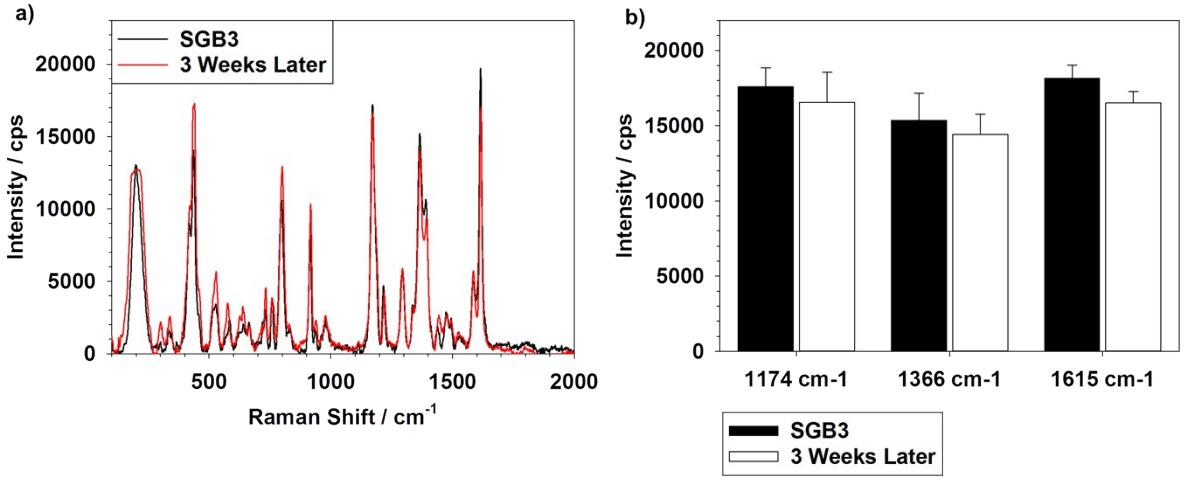

Figure S15. Time-dependent stability of SGB3. After synthesis, SGB3 was stored in the desiccator at room temperature and MGITC was used to obtain the SERS signal.

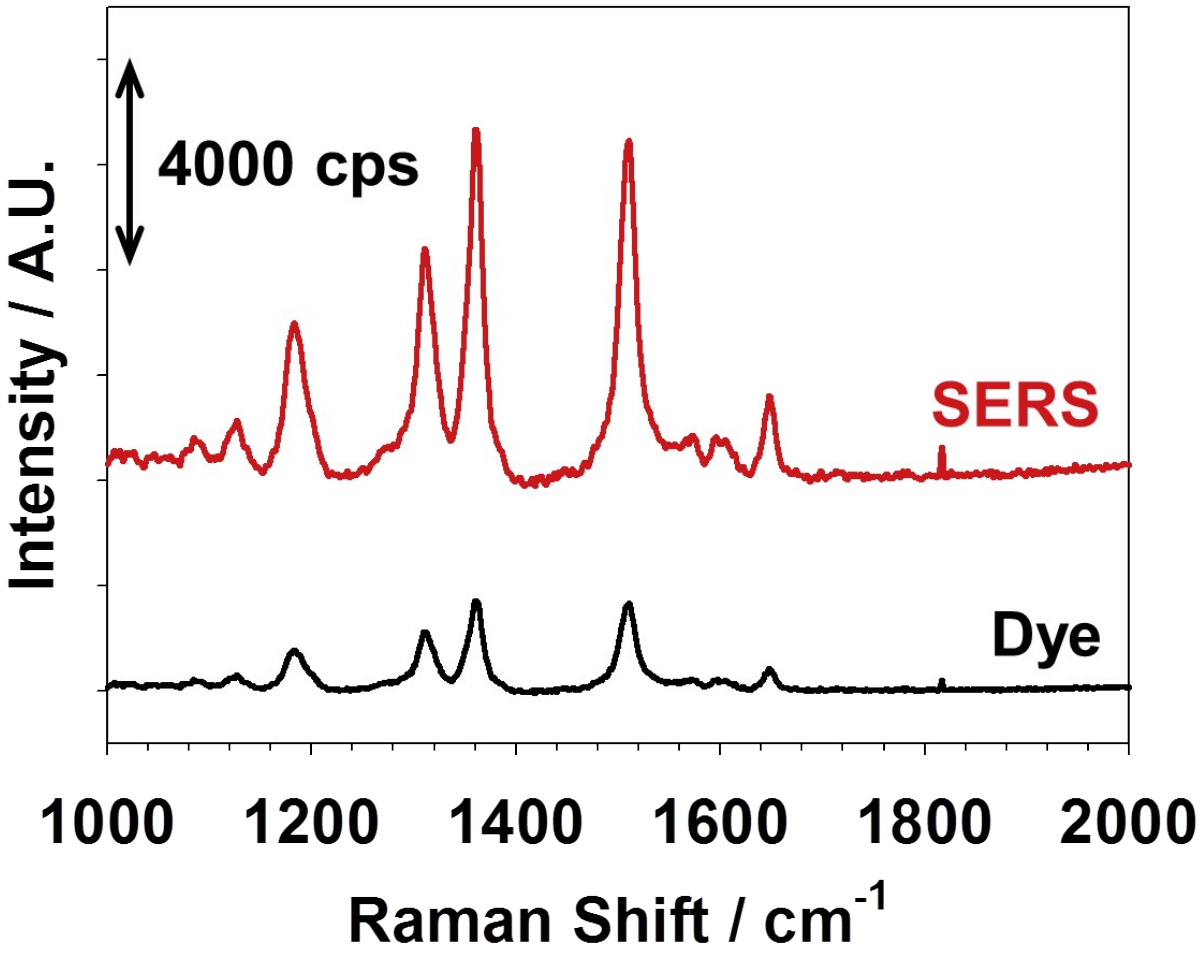

Figure S16. SERS spectra of rhodamine 6G adsorbed on a SGB3 SERS substrate and on a planar Si surface. The intensity ratio of the two spectra implies an enhancement factor of ~10^9.

	at 1312 cm^{-1}	at 1361 cm^{-1}	at 1510 cm^{-1}
I_{SGB3}	4625.89 ± 210.1	7031.1 ± 543.1	6613.2 ± 462.1
I_{Dye}	824.94 ± 76.1	1483.2 ± 211.3	1384.2 ± 201.3
N_{SGB3} per unit area	5.2 x 10^6 molecules		
N_{Dye} per unit are	4.9 x 10^{15} molecules		

Table 1. The relative Raman Intensity at distinct peak position of reporter molecules and estimated number of Raman dyes in calculating EF values of the synthesized substrate.

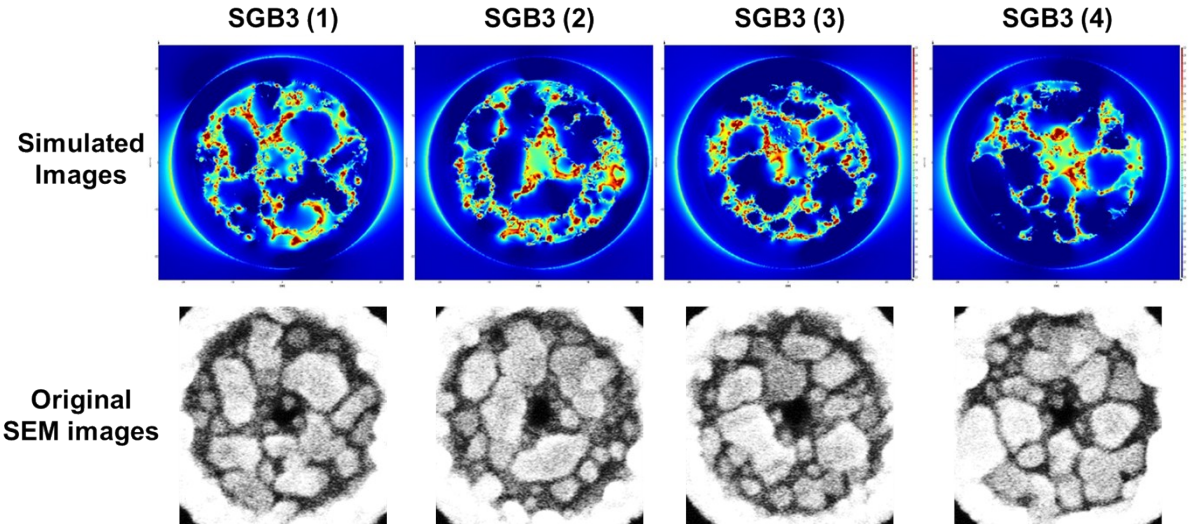

Figure S17. FDTD (Finite Difference Time Domain)-simulated EM field distributions of SGB3 and their original SEM images.

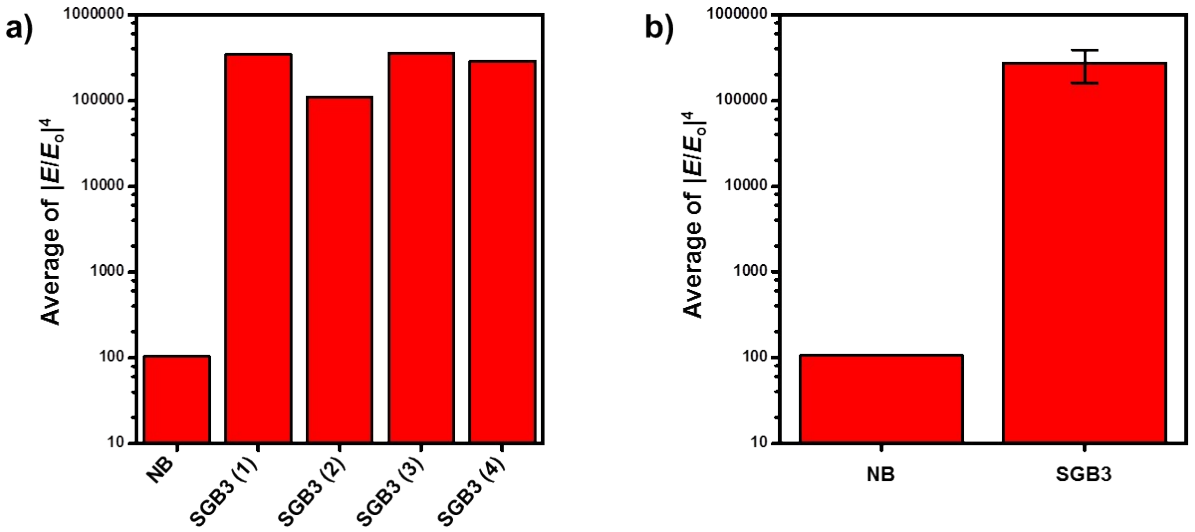

Figure S18. Average $|E/E_0|^4$ values for a) individual NB and SGB3 and b) their average values obtained from the entire area of the field contours in Figure 4 and Figure S12.

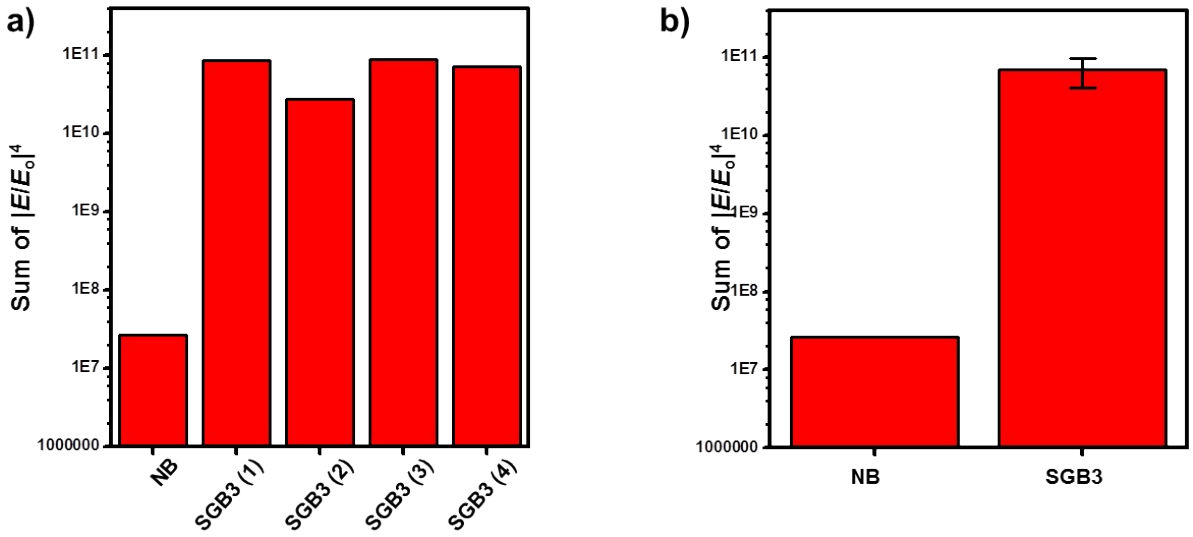

Figure S19. Sum of $|E/E_0|^4$ values for a) individual NB and SGB3 and b) their average values obtained from the entire area of the field contours in Figure 4 and Figure S12.

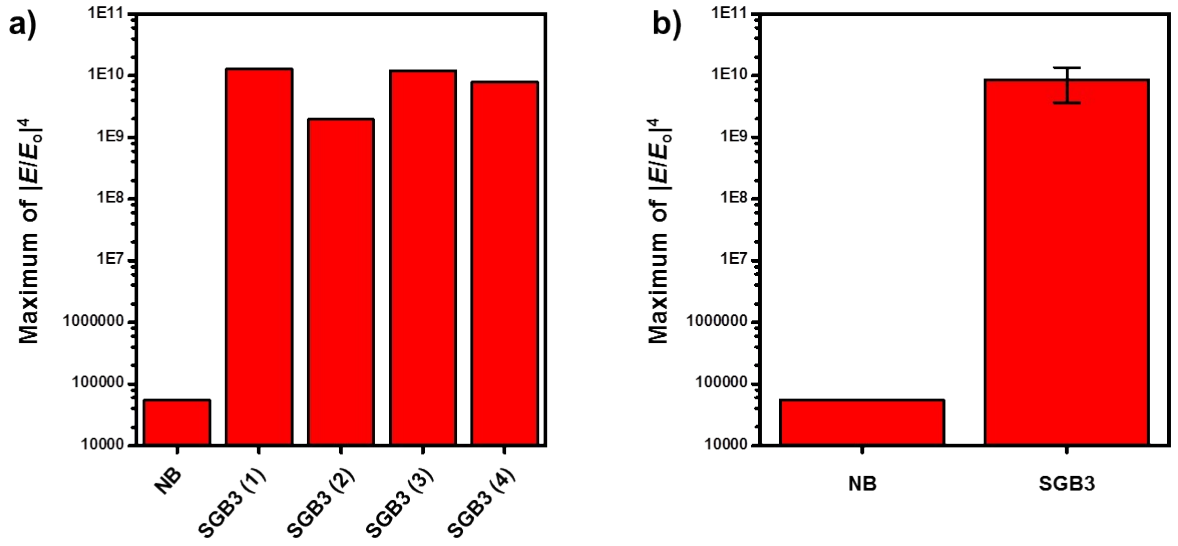

Figure S20. Maximum of $|E/E_0|^4$ values for a) individual NB and SGB3 and b) their averaged values obtained from the entire area of the field contours in Figure 4 and Figure S12.

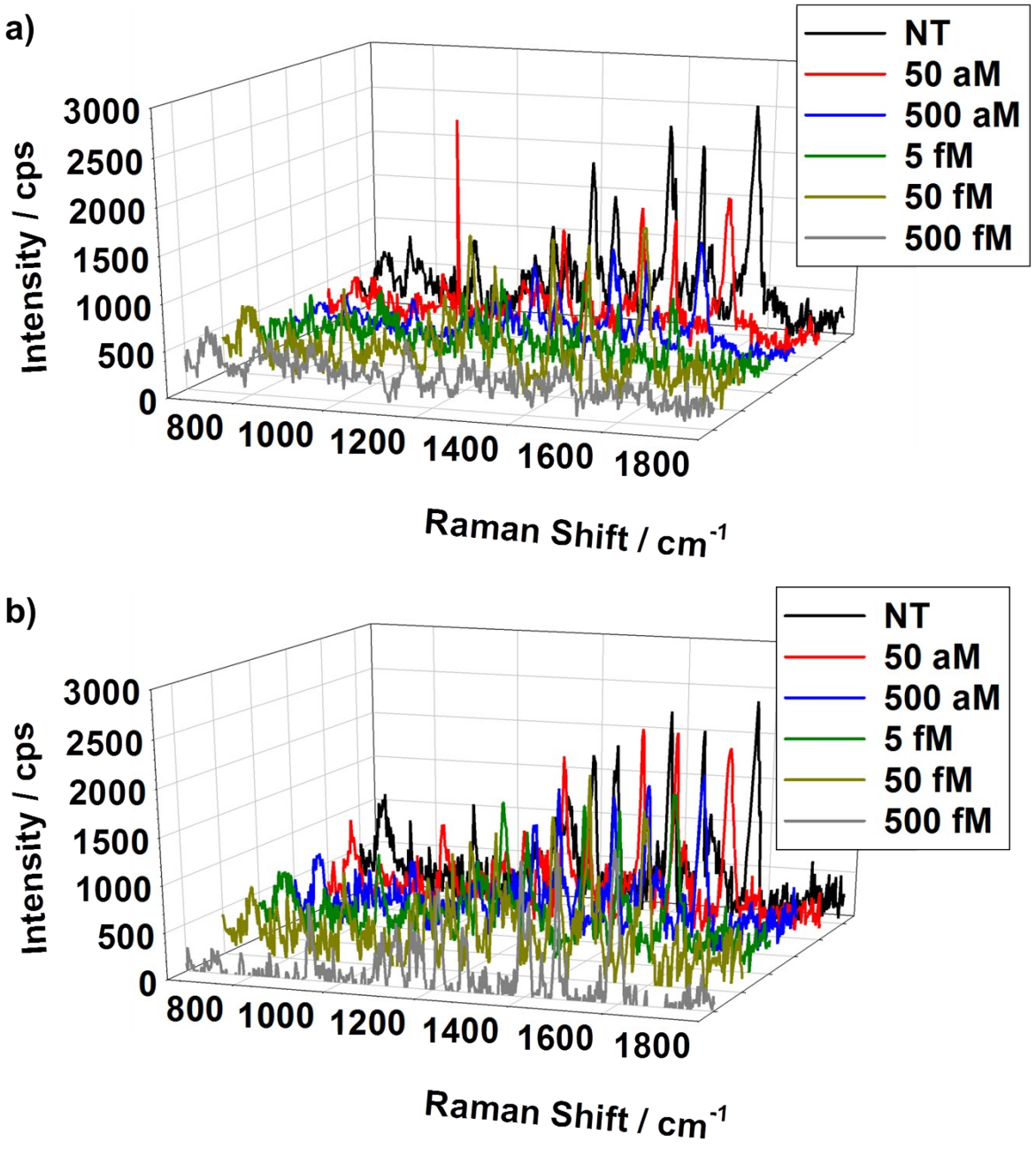

Figure S21. SERS spectra of a) miR-34a molecular beacon and b) mutated miR-34a molecular beacon-immobilized SGB3 treated with different concentrations of target miR-34a.

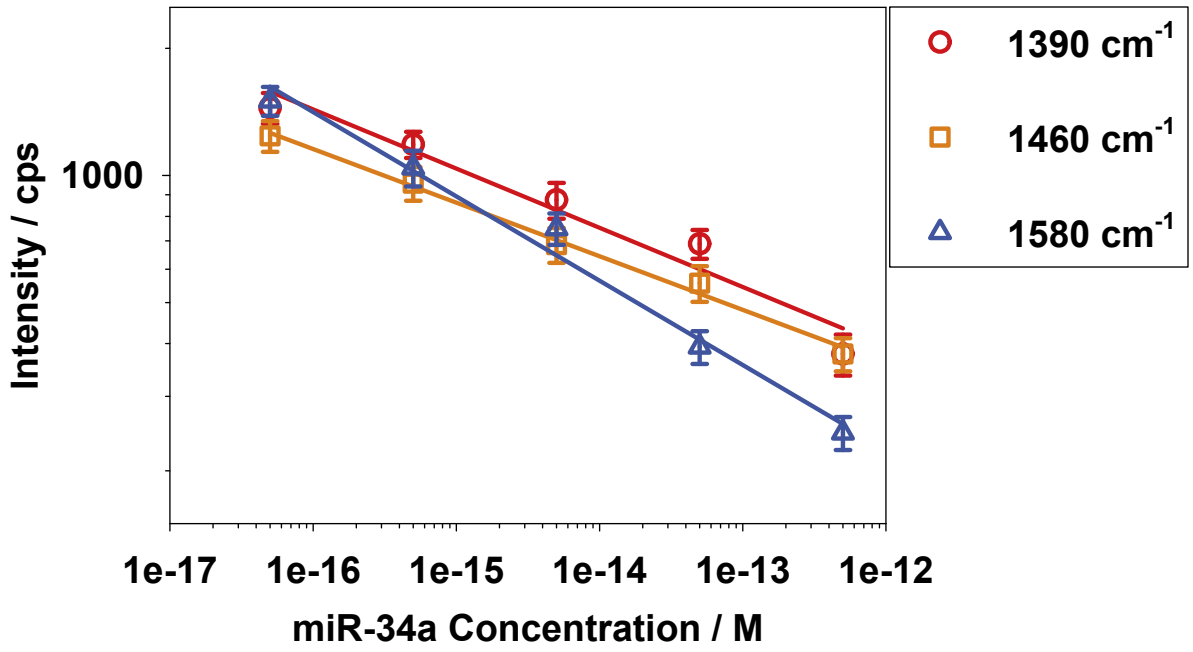

Figure S22. Calibration curve of miR-34a detection with miR-34a molecular beacon where SERS intensity at 1390, 1460, and 1580 cm^{-1} in SGB3 corresponded to Cy3 peaks in MB against various miR-34a logarithmic concentrations. The laser (λ = 633 nm) on the SGB3 was 111 W/mm^2. For the statistical data, 5 random points in SGB3 were measured for each concentration.

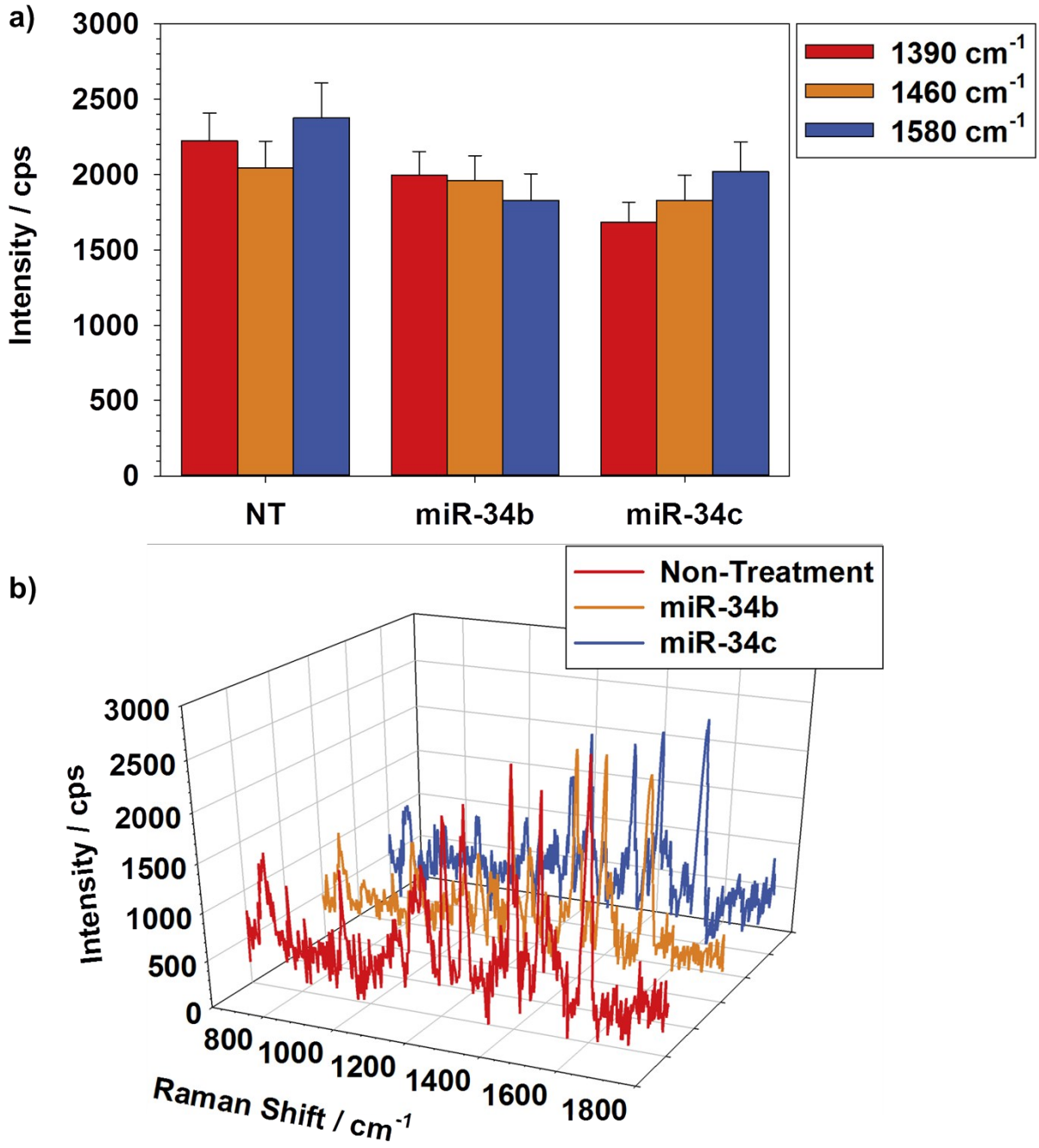

Figure S23. a) Raman signal intensity at 1390, 1460, and 1580 cm^{-1} and b) SERS spectra of miR-34a molecular beacon-immobilized SGB3 before and after treatment with miR-34b or miR-34c. These results suggest that miR-34a MB-modified SGB3 can selectively detect miR-34a. The laser (λ = 633 nm) on the SGB3 was 111 W/mm^2. For statistical data, five random points in SGB3 were measured for each concentration.

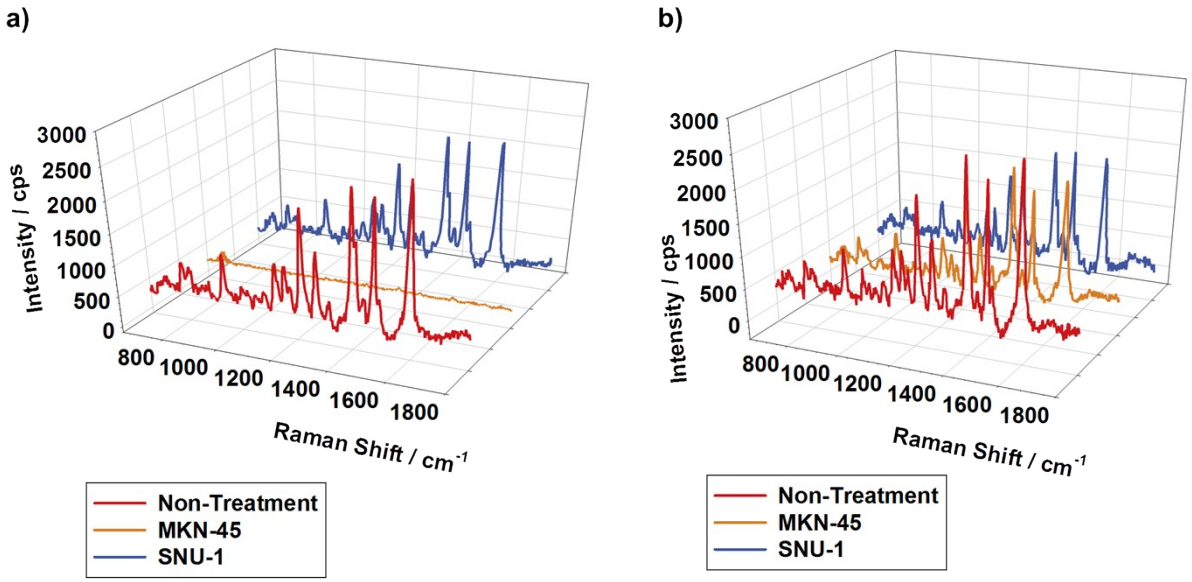

Figure S24. SERS spectra of a) miR-34a molecular beacon and b) mutated miR-34a molecular beacon-immobilized SGB3 treated with MKN-45 and SNU-1 cell lysates.

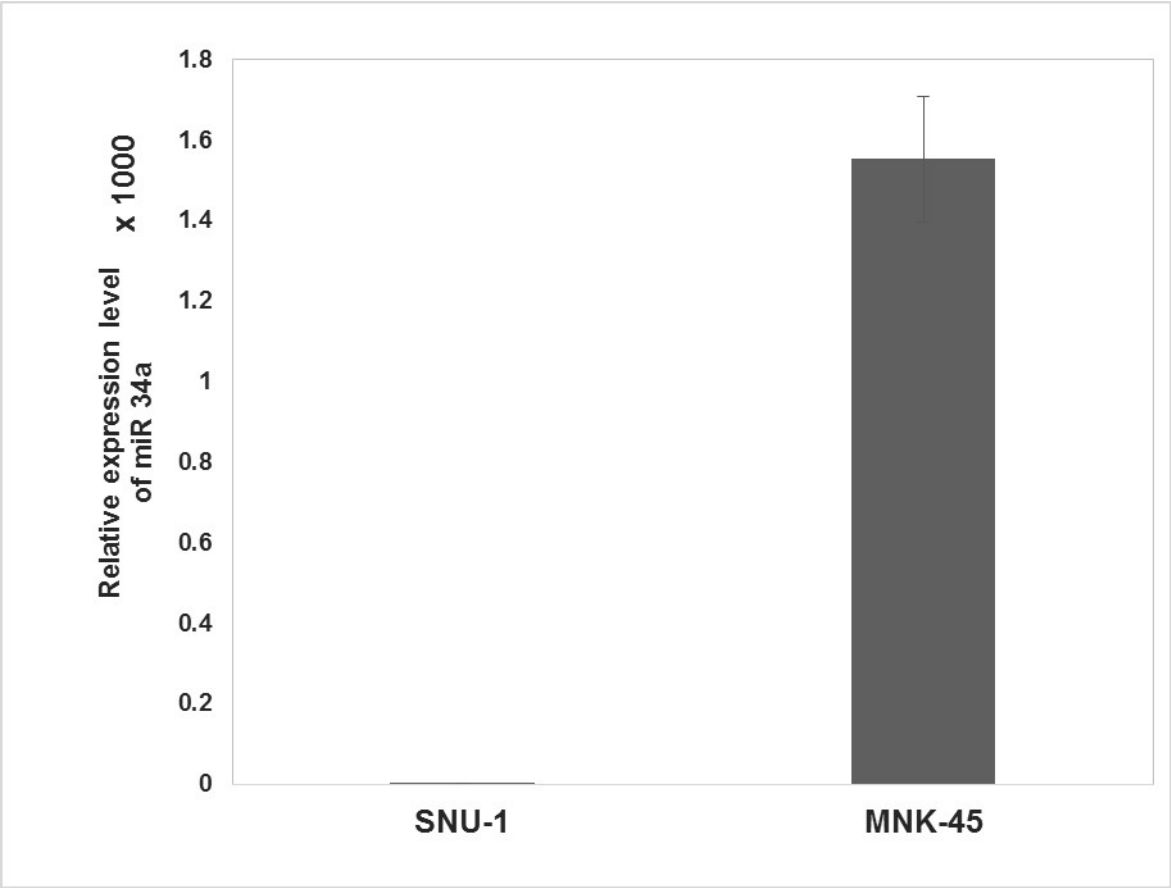

Figure S25. Relative quantification of miR34a by qRT-PCR in human gastric carcinoma cell line, SNU-1 and MKN-45.